Dynamical Methods for Reconstructing the Large Scale Galaxy Density and Velocity Fields

Martin Hendry

University of Glasgow, Glasgow, UK

1 Introduction

Over the past decade the study of the large scale structure of the Universe from analysis of galaxy redshift surveys has matured into an important and highly active area of cosmological research. Redshift surveys have become a powerful tool for probing both the dynamics of galaxy motions on large scales and the nature of the background cosmological model in which the galaxies are embedded. Indeed it is precisely the relationship between these two aspects of redshift surveys – galaxy dynamics and the background cosmology – which is the main focus of this article. While we will see that the subject is firmly rooted in gravitational dynamics, a continuous, fluid, description is preferred to a discrete n-body treatment: galaxies are regarded as tracers of a smooth, underlying density and velocity field, and these fields are in turn treated as smooth perturbations on the background homogeneous and isotropic cosmological model.

The aim of this article is to describe some of the techniques which have recently been developed to reconstruct the galaxy density and velocity fields on large scales, and to use these reconstructed fields to place constraints on the parameters of the underlying cosmological model. Since this topic lies somewhat removed from the research fields of many participants at this meeting, and perhaps many readers of this monograph, the approach of this article will be didactic, with the focus on the reconstruction methods and their context – discussed from first principles – rather than on specific results. We will set out to answer three basic questions:

- What are galaxy redshift surveys?
- Why are they (cosmologically) interesting?
- How do we extract useful cosmological information from them?

2 What are galaxy redshift surveys?

Figure 1 shows a representation of the so-called *Lick map* of the projected galaxy distribution in the nearby Universe, displaying the angular positions of about one million galaxies in the Northern hemisphere (Seldner et al. 1977). It is clear that the galaxy distribution across the sky is far from uniform: one sees a complex pattern of clusters, as well as regions which are almost devoid of galaxies.

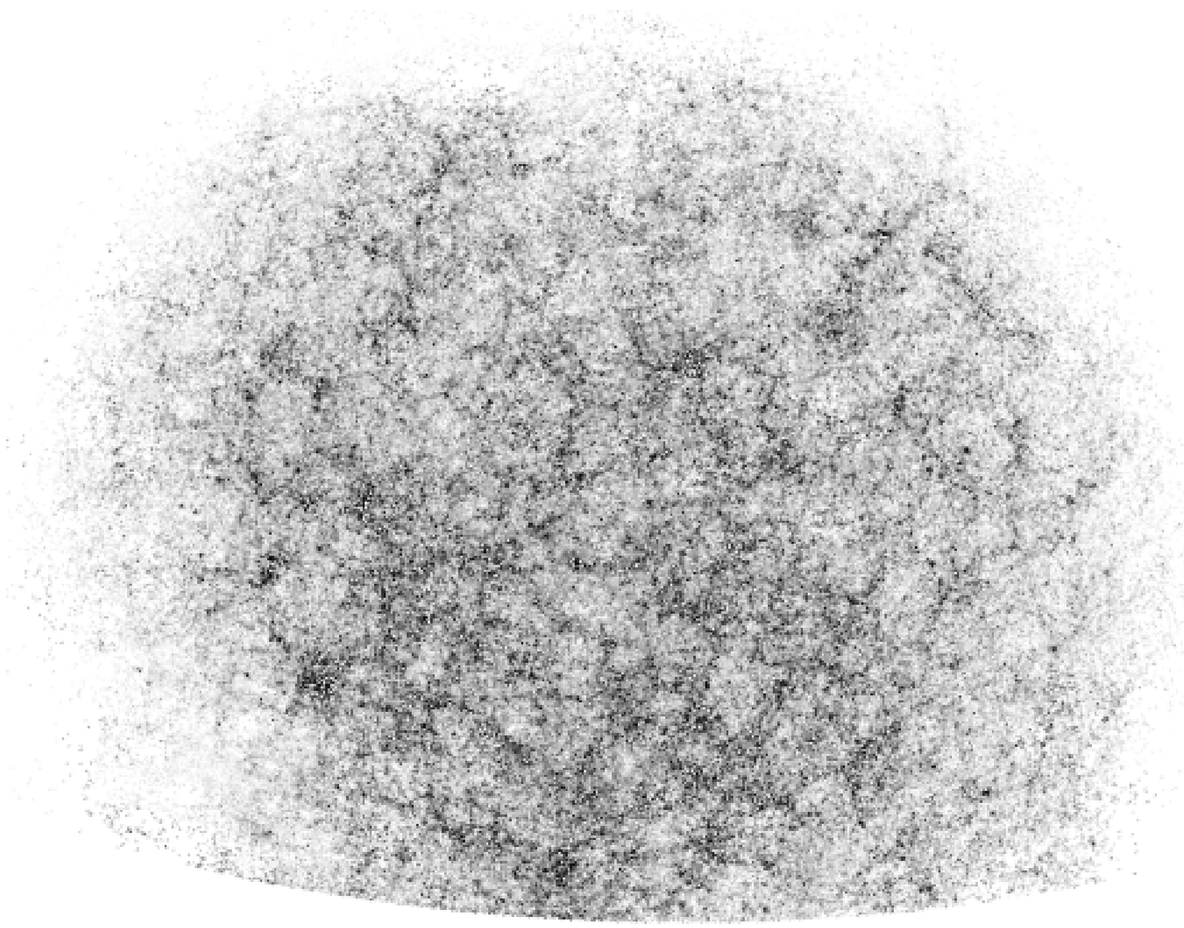

Figure 1. *Representation of the Lick map, showing the projected galaxy distribution of about one million galaxies in the northern hemisphere. Adapted from Peebles (1993)*

In the same way as the distribution of stars in the night sky has been assembled into a pattern of constellations which are mere optical illusions, one must ask if the projected galaxy patterns in the Lick map, and later projected surveys such as the APM galaxy catalogue (Maddox et al. 1990), are merely a line of sight projection effect, or if they reflect the 3-D spatial distribution of galaxies.

Application of the *Copernican principle* (which broadly speaking states that there should be nothing special about our place in – and viewpoint of – the Universe) implies that the clustering which one observes in the projected galaxy distribution should also be present in the 3-D distribution. Indeed, since the 1970s there has been a major research effort in cosmology to use the statistical properties of the 2-D angular galaxy distribution to infer the 3-D spatial distribution, under certain simplifying assumptions (see for example Groth and Peebles 1977). What is clearly desirable, however, is a direct probe of the 3-D spatial galaxy distribution; such a probe is provided by galaxy redshift surveys.

Edwin Hubble's observation of a linear relationship between the estimated distance and radial velocity of recession of nearby galaxies (Hubble 1929) revealed the expansion of the Universe and gave birth to modern cosmology. More straightforwardly Hubble's law also provided us with a simple means to estimate accurately the distance of galaxies on cosmological scales. As any elementary textbook on cosmology will teach us, the linear relation

$$cz = v_{\rm rec} = H_0 d \tag{1}$$

connecting the redshift, z, (deduced from e.g. the wavelength shift of emission lines in the spectrum of a galaxy), radial velocity, $v_{\rm rec}$, and distance, d, is an excellent description on scales of up to several hundred Mpc. The constant of proportionality – the Hubble constant – has a long and colourful history, featuring until quite recently a "factor of two" controversy in its measured value (see e.g. Hendry 1997; Mould et al. 2000). Nevertheless, irrespective of the true value of H_0, the measured redshift of two distant galaxies is certainly a reliable estimator of their relative distance.

In short, then, a redshift survey is a 3-D map of the galaxy distribution where the radial coordinate is the measured recession velocity of each galaxy (or the estimated galaxy distance, assuming a value for the Hubble constant).

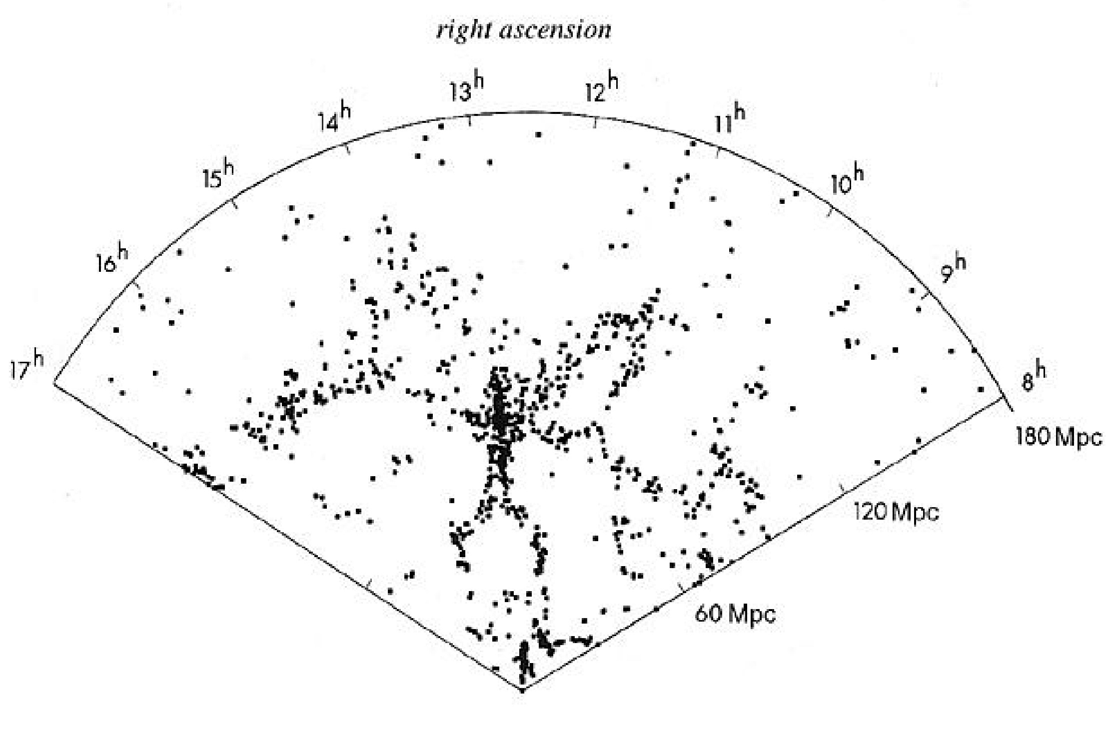

Figure 2. *Slice of the CfA survey of Huchra et al. (1983), showing the distribution in right ascension and distance of around 1000 galaxies.*

The function of galaxy redshift surveys is (at least) twofold. First, they are useful as a purely *cosmographic* tool: by mapping the 3-D positions of galaxies they reveal directly patterns in the distribution which can be only indirectly inferred from the projected distribution. An example of an early redshift survey which made a significant cosmographic impact is the Harvard CfA survey (Huchra et al. 1983), one 'slice' of which – containing about 1000 galaxies – is shown in Figure 2. This picture, from the data of Huchra et al. (1990), shows the right ascension and inferred distance of around 1000 galaxies lying within a 'wedge' on the sky; the thickness (6° in declination) of the wedge has been suppressed in the plot. We can see that the distribution of galaxies in the nearby Universe is characterised by clusters, filamentary structures and voids, with a characteristic size of around 50 Mpc. This was consistent with the findings of earlier 'pencil beam' redshift surveys, which had indicated the existence of large underdense regions (Kirshner, Oemler and Schechter 1978). Note the presence of the coherent filamentary structure which stretches across almost all of Figure 2 at a distance of about 80 Mpc, which has been termed the 'Great Wall' (Geller and Huchra 1989).

Since the CfA survey was first published many more, considerably deeper, slices of the nearby Universe have been mapped in a similar manner (see e.g. Giovanelli and Haynes 1991; Vogeley et al. 1994; Loveday et al. 1996; Shechtman et al. 1996; Vetollani et al. 1997). Among the most recent of these is the 'Two degree field' or 2dF catalogue (Maddox 2000), which is more than an order of magnitude larger in size and depth than the CfA surveys. In the early years of the 21st century, the Sloan Digital Sky Survey (York et al. 2000) will also be completed, generating a catalogue of one million galaxy redshifts across approximately one quarter of the sky. Interestingly, however, the largest observed features in these much later and deeper surveys are still comparable in size to those shown in Figure 2 – indicating that on very large scales the Universe begins to look homogeneous, as predicted by the *cosmological principle*.

Around the same time as first results from 'slice' surveys such as the CfA were being presented, systematic programmes of studying *all-sky* redshift surveys were also being developed (Rowan Robinson et al. 1990; Yahil et al. 1991) – chiefly making use of the (almost) all-sky coverage of the infra-red sky in galaxy maps compiled by the IRAS Infra-Red astronomical satellite, launched in 1983. As we will see in the next section, it is all-sky surveys which will be the main concern of this article.

3 Why are redshift surveys interesting?

3.1 Statistical analysis of galaxy clustering

The statistical analysis of large galaxy redshift surveys is, in itself, a powerful cosmological probe, meriting a lengthy review article in its own right. This is because the observed pattern of galaxy clustering can be directly related to the parameters of the underlying cosmological model. Over the past few decades a very extensive battery of statistical techniques have been developed to extract cosmological information from the analysis of galaxy clustering. These techniques include (with representative references): n point correlation functions (Davis and Peebles 1983), galaxy counts-in-cells (Balian and Schaefer 1989), void probability functions (White 1979), Voronoi tesselations (van de Weygaert and Icke 1989), power spectra (Peacock and Dodds 1994), redshift distortions (Kaiser

1987; Hamilton 1998), spherical harmonic analyses (Scharf and Lahav 1993), percolation and multifractal methods (Klypin and Shandarin 1993), Minkowski functionals (Kerscher et al. 1997), minimal spanning trees (Krzewina and Saslaw 1996) and the genus and other topological measures (Bardeen et al. 1986). Lack of space forces us to avoid further discussion of these statistical techniques and instead to restrict our consideration to methods which make explicit use of *dynamical* information from redshift surveys. Such a distinction between galaxy clustering and galaxy dynamics is rather artificial, however, since (as we will see in Section 3.3) the spatial distribution and motions of galaxies are inextricably connected within the *gravitational instability paradigm* – the standard theoretical framework for the formation of structure in the Universe. For a detailed review of how the statistics of galaxy clustering can be used as a cosmological probe, the reader is referred to e.g. Strauss and Willick (1995).

3.2 Cosmology from galaxy dynamics: overture

To understand fully the dynamical usefulness of all-sky redshift surveys requires the theoretical background which we will review in the next section. The essence of their usefulness is easily seen, however.

In the gravitational instability paradigm, the observed radial velocity of a distant galaxy is not simply due to the Hubble expansion, but also includes a contribution from the *local* motions induced by the gravitational attraction of matter around the galaxy. This additional motion, known as the galaxy's radial *peculiar* velocity, distorts the positions of galaxies in a redshift survey compared with their true radial positions in space. Whilst for distant galaxies (e.g. $r \geq 100$ Mpc) the contribution of the peculiar velocity to the total observed recession velocity becomes increasingly small and can be safely ignored, on smaller scales peculiar velocities can be significant – not least because they do not represent a random 'error' added to the Hubble expansion velocity, but rather a systematic pattern of deviations from a linear Hubble law which is coherent over large volumes of space. This is because these distortions – far from being peculiar – are exactly what one would predict within the gravitational instability framework: that structure forms through the evolution of density inhomogeneities, which move and grow under the influence of gravity.

Examples of early studies of such large scale galaxy flows, from comparing observed galaxy redshifts with estimated galaxy distances (see also Section 4.8), include the detection of 'Virgocentric flow' of the Milky Way towards the nearby Virgo Cluster of galaxies (Aaronson et al. 1982) and the discovery of a streaming motion, coherent over more than 100 Mpc, towards the direction of the constellations Hydra and Centaurus, interpreted as evidence for a mass concentration which was termed the 'Great Attractor' (Dressler et al. 1987).

The gravitational instability theory of structure formation allows one to relate the distribution of galaxies in an all-sky redshift survey to their peculiar motions. Moreover, the relationship between the spatial distribution and motions of galaxies (or at least the matter, from which the galaxies form) depends on the underlying cosmological model in which the galaxy distribution is moving and evolving. This, then, highlights the second function of galaxy redshift surveys: they are also a *cosmological* tool – i.e. the galaxy distribution can be used to place constraints on parameters of the underlying cosmological model.

3.3 Friedmann's equations and the evolution of the scale factor

In this section we briefly review the essential theoretical elements which relate the parameters of cosmological models to the formation of structure in the Universe under the influence of gravity. There is a vast literature on this subject, with dozens of excellent textbooks and review articles. References which are particularly relevant to the theme of velocity and density reconstruction include Strauss and Willick (1995), Peacock (1999) and Dekel and Ostriker (1999), and the interested reader is directed to these references for a more detailed (and in some places more rigorous!) introduction to this topic.

In the standard Big Bang model of cosmology the evolution of the Universe is described in terms of the *Friedmann-Robertson-Walker* (FRW) homogeneous and isotropic background model, with line element (describing the interval between two neighbouring points in spacetime) given by (in spherical polar coordinates)

$$ds^2 = c^2dt^2 - a(t)^2\left[\frac{dr'^2}{1-kr'^2} + r'^2(d\theta^2 + sin^2\theta d\phi^2)\right] \tag{2}$$

Here k is the *curvature constant*, which takes the value -1, 0, and 1 for a Universe with negative, zero and positive spatial curvature respectively. The function $a(t)$ denotes the *scale factor* of the Universe, which is a measure of the typical physical separation of e.g. galaxies as a function of time, t, since the Big Bang. The coordinate triple (r', θ, ϕ) denotes *comoving* coordinates – i.e. coordinates which expand with the background Universe. Thus, in the limit of a completely homogeneous and isotropic Universe, the comoving separation of two points in spacetime does not change with time, while the *proper distance*, r, between them is given by

$$r = a(t)f(r') \tag{3}$$

where

$$f(r') = \begin{cases} \sin^{-1} r' & \mathrm{k} = 1, \\ r' & \mathrm{k} = 0, \\ \sinh^{-1} r' & \mathrm{k} = -1 \end{cases} \tag{4}$$

The dynamical evolution of the scale factor can be determined from the solution of Einstein's equations, assuming the FRW metric of eq. (2) and treating the mass-energy content of the Universe as a perfect fluid, with density, ρ, and pressure, P, (usually assumed to be zero). One obtains the following two equations for $a(t)$

$$\frac{\ddot{a}}{a} = -\frac{4}{3}\pi G(\rho + \frac{3P}{c^2}) + \frac{\Lambda c^2}{3} \tag{5}$$

and

$$\left(\frac{\dot{a}}{a}\right)^2 = \frac{8\pi}{3}G\rho + \frac{\Lambda c^2}{3} - \frac{kc^2}{a^2} \tag{6}$$

Here Λ is the *cosmological constant*, introduced by Einstein to allow a static solution for $a(t)$. The Hubble parameter is defined as $H \equiv \dot{a}/a$, with present day value (i.e.

evaluated at time $t = t_0$) given by H_0, which is of course the constant of proportionality in eq. (1). For $\Lambda = 0$ then

$$k = 0 \Leftrightarrow \rho = \rho_{\rm crit} = \frac{3H^2}{8\pi G} \tag{7}$$

where $\rho_{\rm crit}$ is the *critical density* which marks the division between a Universe which will expand indefinitely and one which will eventually recollapse. The dimensionless matter density, Ω_m, is defined as

$$\Omega_m = \frac{\rho}{\rho_{\rm crit}} = \frac{8\pi G\rho}{3H^2} \tag{8}$$

which is, in general, time dependent due to the time dependence of ρ and H. We denote by Ω_{m0} the present day value of the density parameter. It is also customary to define

$$\Omega_\Lambda = \frac{\Lambda c^2}{3H^2} \tag{9}$$

which denotes the (time-dependent, through H) contribution of the cosmological constant to the dimensionless density parameter. The generic prediction of inflationary cosmological models (Kolb and Turner 1990; Liddle and Lyth 2000), which undergo a period of very rapid (i.e. exponential) expansion during early times, is that the Universe has zero curvature (i.e. $k = 0$) from which it is straightforward to show that

$$\Omega_m + \Omega_\Lambda = 1 \tag{10}$$

although the relative importance of Ω_m and Ω_Λ changes as the Universe evolves.

There has been much recent interest in the cosmological literature in attempts to measure the values of Ω_{m0} and $\Omega_{\Lambda 0}$ from the *Hubble diagram* of distant supernovae and the pattern of temperature fluctuations in the cosmic microwave background radiation (CMBR), the relic radiation from the Big Bang which emanates from the 'surface of last scattering': the epoch when the Universe was hot enough to ionise neutral hydrogen, thus rendering it effectively opaque due to scattering of photons by free electrons. For further discussion of this exciting new area of research, see e.g. White, Scott and Silk (1994), Lineweaver (1997), Perlmutter et al (1999) and Tegmark and Zaldarriaga (2000). In this article, however, we will restrict our attention to methods for estimating the (present day) dimensionless matter density, Ω_{m0}, from redshift surveys, and for notational convenience we will henceforth denote Ω_{m0} simply by Ω_0.

3.4 How did structure form?

The gravitational instability paradigm is the standard theoretical framework which describes the growth of structure on cosmological scales. It asserts that in the early Universe (e.g. at the epoch of the CMBR, about 300,000 years after the Big Bang) there were already present small perturbations in the density of matter. The origin of these perturbations need not concern us here, although in most scenarios they are 'imprinted' on the microwave background from a much earlier epoch – e.g. due to quantum fluctuations during the inflationary phase of the Universe (see e.g. Liddle and Lyth 2000). What is important is that the density perturbations grow under the influence of gravity, and essentially one needs to consider no physical processes other than gravity in order to explain the distribution and motion of the matter as the Universe evolves.

The problem is most readily treated using a fluid description (e.g. Weinberg 1972; Coles and Lucchin 1993; Peacock 1999), i.e. we define a (scalar) mass density field $\rho = \rho(\mathbf{r}, t)$ and (vector) velocity field $\mathbf{V} = \mathbf{V}(\mathbf{r}, t)$ as a function of position, $\mathbf{r}$ (in proper coordinates), and cosmic time, t. (Note that, unlike the homogeneous background cosmology, the density is now a function of position. Note also that $\mathbf{V}$ includes the Hubble expansion at $\mathbf{r}$). The time evolution of ρ and $\mathbf{V}$ will, then, be described by the following equations

$$\frac{\partial \rho}{\partial t} + \nabla_r \cdot (\rho \mathbf{V}) = 0 \tag{11}$$

$$\frac{\partial \mathbf{V}}{\partial t} + (\mathbf{V} \cdot \nabla_r)\mathbf{V} + \nabla_r \phi = 0 \tag{12}$$

and

$$\nabla_r^2 \phi = 4\pi G \rho \tag{13}$$

where ∇_r denotes the gradient operator in proper coordinates. These are, respectively, the equation of continuity, equation of motion and Poisson equation for the fluid, with (scalar) gravitational potential $\phi = \phi(\mathbf{r}, t)$.

If we consider galaxies observed today in the nearby Universe as tracers of the velocity field, $\mathbf{V}$, the observed line of sight recession velocity (equal to the radial component of $\mathbf{V}$) of a galaxy at position $\mathbf{r}$ is given by

$$v_{\mathrm{rec}} = H_0 r + \hat{\mathbf{r}} \cdot [\mathbf{v}(\mathbf{r}) - \mathbf{v}_0] \tag{14}$$

Here $\mathbf{v}(\mathbf{r})$ is the peculiar velocity at position $\mathbf{r}$, $\hat{\mathbf{r}}$ is a unit vector in the direction of the observed galaxy and $\mathbf{v}_0$ is the peculiar velocity of our location with respect to the reference frame in which the temperature distribution of the CMBR appears isotropic – i.e. the reference frame comoving with the mean motion of galaxies in the local Universe. We can determine this peculiar velocity if we assume that it produces the observed dipole anisotropy in the CMBR (Fixsen et al. 1994; Lineweaver et al. 1996). Correcting for this peculiar velocity is usually referred to as correcting observed galaxy redshifts to the 'CMBR frame'.

We next define the *dimensionless density contrast*, δ

$$\delta(\mathbf{r}, t) = \frac{\rho(\mathbf{r}, t) - \overline{\rho}(t)}{\overline{\rho}(t)} \tag{15}$$

where $\overline{\rho}(t)$ is the mean mass density of the background FRW model.

Expanding eqs. (11) and (12) to first order in δ and $|\mathbf{v}|$, converting the gradient operator to comoving coordinates and subtracting the zeroth order solution for the background model leads to the following equations

$$\frac{\partial \delta}{\partial t} + \frac{1}{a} \nabla \cdot \mathbf{v} = 0 \tag{16}$$

and

$$\frac{\partial \mathbf{v}}{\partial t} + \frac{\dot{a}a}{\mathbf{v}} + \frac{1}{a} \nabla \phi = 0 \tag{17}$$

Taking the time derivative of eq. (16) , the divergence of eq. (17) and substituting into eq. (13) gives

$$\frac{\partial^2 \delta}{\partial t^2} + 2\frac{\dot{a}}{a}\frac{\partial \delta}{\partial t} = 4\pi G \overline{\rho} \delta \tag{18}$$

We seek a solution which is separable in its spatial and time dependence, of the form

$$\delta = A(\mathbf{r})D_1(t) + B(\mathbf{r})D_2(t) \tag{19}$$

where D_1 and D_2 are respectively growing and decaying modes (i.e. D_1 grows and D_2 decays as the scale factor increases).

A simple, analytic solution for δ exists in special cases, for example the *Einstein de Sitter* model with $\Omega_0 = 1$ and $\Lambda = 0$. In this case it is easy to show that $a(t) \propto t^{2/3}$. Mass conservation implies that $\overline{\rho} \propto a(t)^{-3}$, which then reduces eq. (18) to

$$\frac{\partial^2 \delta}{\partial t^2} + \frac{4}{3t}\frac{\partial \delta}{\partial t} = \frac{2}{3t^2}\delta \tag{20}$$

This has analytic solution

$$\delta(\mathbf{r}, t) = A(\mathbf{r})t^{2/3} + B(\mathbf{r})t^{-1} \tag{21}$$

For more general cosmological models, the solution for δ depends on the value of Ω_0 and Ω_Λ. At late times the second term in this solution becomes negligible, so that eq. (16) reduces to

$$\nabla \cdot \mathbf{v} = -a\delta \frac{\dot{D}_1}{D_1} = -a_0 H_0 f \delta \tag{22}$$

where the *growth factor*, f, is given by

$$f \equiv \frac{1}{H_0 D_1}\frac{dD_1}{dt} = \frac{d \log D_1}{d \log a} \tag{23}$$

An excellent approximation to f (Lahav et al. 1991) is

$$f(\Omega_0, \Omega_\Lambda) = \Omega_0^{0.6} + \frac{\Omega_\Lambda}{70}\left(1 + \frac{1}{2}\Omega_0\right) \tag{24}$$

from which it follows that (neglecting the very weak Ω_Λ dependence)

$$\delta = -\frac{\nabla \cdot \mathbf{v}}{a_0 H_0 \Omega_0^{0.6}} \tag{25}$$

Eq. (25) may be solved using standard techniques from the theory of electrostatics, to give

$$\mathbf{v}(\mathbf{r}) = \frac{H_0 \Omega_0^{0.6}}{4\pi} \int \frac{d^3 r' \delta(\mathbf{r}')(\mathbf{r}' - \mathbf{r})}{|\mathbf{r}' - \mathbf{r}|^3} \tag{26}$$

Equations (25) and (26) epitomise the theme of this article: in the gravitational instability paradigm there is a precise relationship between the density field and peculiar velocity field of matter, and that relationship depends on the parameters of the background cosmological model. Thus, if we use the distribution and motions of galaxies to reconstruct the matter density and velocity fields, we can in turn use these dynamical fields to place constraints on the background cosmological parameters.

The importance of all-sky redshift surveys in this reconstruction process is seen from eq. (26), where the integral formally is over all space. In other words, the peculiar velocity field at a given position is not simply induced locally, but results from the mass distribution in a large surrounding volume. Thus, simply ignoring the contribution from a particular region of the survey volume, due to e.g. poor sampling, will result in systematic errors in the reconstructed dynamical fields.

The theoretical framework presented thus far is a simplification in several key respects, and the remainder of this article is concerned with how that simplified picture is handled in practice. Specifically, we must address the following points:

- We measure galaxy redshifts, not positions, but eq. (26) is an integral over spatial positions.
- Our theoretical framework treats δ and $\mathbf{v}$ as smooth fields, following a fluid description. We use galaxy redshift surveys to trace δ and $\mathbf{v}$, but our tracers are only a sparse and noisy sample of those fields.
- The analysis which leads to eqs. (25) and (26) assumes linear perturbation theory. In practice we must deal with a density field which has evolved (at least on small scales) well beyond the linear regime.
- δ measures the overdensity in the distribution of *mass*, whereas redshift surveys measure the distribution of galaxies. The relationship between the galaxy and mass distribution may be (and again, at least on small scales, clearly is!) non-trivial.

Despite these caveats, the essence of eqs. (25) and (26) is a simple, and rather profound idea: that the dynamics of galaxies can tell us something of the nature of the Universe in which we live – determining, for example, whether the Universe will eventually recollapse or continue expanding indefinitely. One should not lose sight of this far-reaching result, while recognising – as we will see in the following sections – that the devil is in the detail.

4 How do we extract information from surveys?

4.1 Iterative reconstruction methods

A common methodology adopted in attempting to recover cosmologically useful information from all-sky redshift surveys is to solve eq. (26) in *real* space iteratively in a self-consistent manner. The procedure adopted is essentially as follows.

1. Estimate a smooth $\delta(\mathbf{r})$ from the observed distribution of galaxies in the redshift survey, assuming first that $cz = r$ – i.e. ignoring the distorting effect of galaxy peculiar motions.
2. Using eq. (26), compute the peculiar velocity field, $\mathbf{v}(\mathbf{r})$, predicted by the assumed $\delta(\mathbf{r})$.
3. Use the radial components of the predicted velocity field to correct the 'observed' values of the smoothed density field at each position, $\mathbf{r}$.
4. Repeat iteratively from step (2) until convergence is reached

This iterative reconstruction procedure has been applied to a number of different redshift surveys, including for example the IRAS 1.9Jy and 1.2Jy surveys (Strauss et al. 1992; Fisher et al. 1995a), the QDOT survey (Kaiser et al. 1991), Optical Redshift Survey (Santiago et al. 1995) and, recently, the IRAS PSCz survey (Branchini et al. 1999). Other notable implementations of this iterative scheme, for various galaxy surveys and catalogues, include Hudson (1993), Freudling et al. (1994) and Teodoro (1999).

4.2 The impact of sparse sampling

Sparse sampling of the galaxy distribution throughout the volume of the redshift survey introduces random 'shot noise' in the reconstruction. This can to some extent be controlled by filtering of the smoothed galaxy density field, using e.g. the *Wiener filter*, which minimises the variance between the reconstructed and true density fields (Wiener 1949). Further discussion of this topic lies beyond the scope of these lectures, but the reader is referred to Fisher et al. (1995b) for more details. It is worth noting in passing, however, that the QDOT survey (Rowan Robinson et al. 1990) confronted directly the issue that galaxies are only discrete tracers of the underlying dynamical fields, and made something of a virtue of a sparse sampling strategy, designed to optimise the efficiency of the survey. In other words, instead of obtaining redshifts for every relevant galaxy within a given volume of the local Universe, the QDOT strategy was to sample only a fixed fraction of galaxies, sufficient to reconstruct iteratively the dynamical fields without substantial loss of cosmological information, while allowing the survey to probe a much larger volume – albeit only sparsely.

More serious than 'shot noise' effects are variations in the sampling with redshift and/or direction, both of which introduce *systematic* errors in the reconstructed density and velocity fields.

4.3 The impact of observational selection effects

While the iterative reconstruction of the dynamical fields is a straightforward idea in principle, its practical implementation is limited by the fact that the integral of eq. (26) is over all space, while redshift surveys are generally *flux-limited* and *masked*. These two effects mean that galaxies, respectively, fainter than a specified limiting observable flux and within a particular 'masked' solid angle on the sky will be excluded from the survey; the two exclusions can be termed together 'observational selection effects', and also pose problems for other, non-iterative, reconstruction procedures, as we will see later.

The presence of a directional mask arises because a redshift survey is never truly 'all-sky', since the observation of e.g. IRAS galaxies behind the plane of the Milky Way is rendered almost impossible by the contaminating effect of dust in our own Galaxy. The IRAS 1.9Jy and 1.2Jy surveys covered 88% of the sky, missing a strip 10° wide around the Galactic plane and high latitude regions inadequately covered by the IRAS satellite. The more recent PSCz survey (Saunders et al. 2000) had similar sky coverage but to a deeper flux limit.

The effect of a flux limit is generally radial rather than directional. It renders the sampling of galaxies increasingly sparse at large distances. This problem is usually addressed by defining a *selection function* for the survey, which measures the probability that a galaxy at a given distance meets the selection criteria to enter the survey catalogue. We can illustrate how a selection function is defined as follows.

Suppose that the luminosity of all galaxies were a constant, $L = L_*$, say. Then, for a flux limit $\mathcal{F}_{\rm lim}$, it follows that a galaxy at distance, r, will be observable provided

$$\frac{L_*}{4\pi r^2} = \mathcal{F} > \mathcal{F}_{\rm lim} \tag{27}$$

or

$$r < r_{\rm lim} = \left(\frac{L_*}{4\pi \mathcal{F}_{\rm lim}} \right)^{1/2} \tag{28}$$

Thus one could in principle sample completely the galaxy distribution within a sphere of radius $r_{\rm lim}$, producing a *volume limited* survey.

In practice, however, galaxy luminosities are not constant but are described by a luminosity function, $\Phi(L)$, such that $\Phi(L)dL$ is proportional to the number density of galaxies with luminosity between L and $L + dL$. Thus for a sharp flux limit at $\mathcal{F}_{\rm min}$ galaxies of different luminosities will 'fade out' at different distances, and the selection function for the survey is a convolution over the galaxy luminosity function. Explicitly, the selection function, $\phi(r)$, is defined as

$$\phi(r) = \frac{\int_{4\pi r^2 \mathcal{F}_{\rm lim}}^{\infty} \Phi(L)dL}{\int_0^{\infty} \Phi(L)dL} \tag{29}$$

The mean galaxy number density, $\overline{n}$, can be estimated from the selection function computed for a discrete sample of galaxies as follows

$$\overline{n} = \frac{1}{V} \sum_{\rm galaxies} \frac{1}{\phi(r_i)} \tag{30}$$

and a smoothed galaxy overdensity field, $\delta_g(\mathbf{r})$, can be constructed from

$$\delta_g(\mathbf{r}) = \frac{1}{\overline{n}} \sum_{\rm galaxies} \frac{W(\mathbf{r} - \mathbf{r}_i)}{\phi(r_i)} - 1 \tag{31}$$

where $W(\mathbf{r} - \mathbf{r}_i)$ is a *window function* which smooths the point galaxy distribution. Examples of window functions commonly used in the literature include a spherical 'top hat' window and Gaussian window (see e.g. Strauss and Willick 1995 for more details).

Thus, the sparse sampling at large distances caused by the flux limit is compensated in the reconstruction procedure by the presence of the selection function 'renormalising' our estimate of the smooth galaxy density field to take account of the 'missing' galaxies. The IRAS 1.9Jy survey mapped the redshifts of 2658 galaxies with 60 micron flux f_{60} brighter than 1.936Jy. The 1.2Jy survey increased this total to 5339 galaxies with $f_{60} \geq 1.2$Jy, and the PSCz survey to 15411 galaxies with $f_{60} \geq 0.6$Jy.

The impact on the reconstruction of incomplete sky coverage, caused by the masking effects of e.g. the galactic plane, must also be taken into account. One approach to this problem is to 'fill in' the masked regions by adding randomly generated galaxies to the redshift survey. Various strategies have been adopted to do this. Yahil et al.

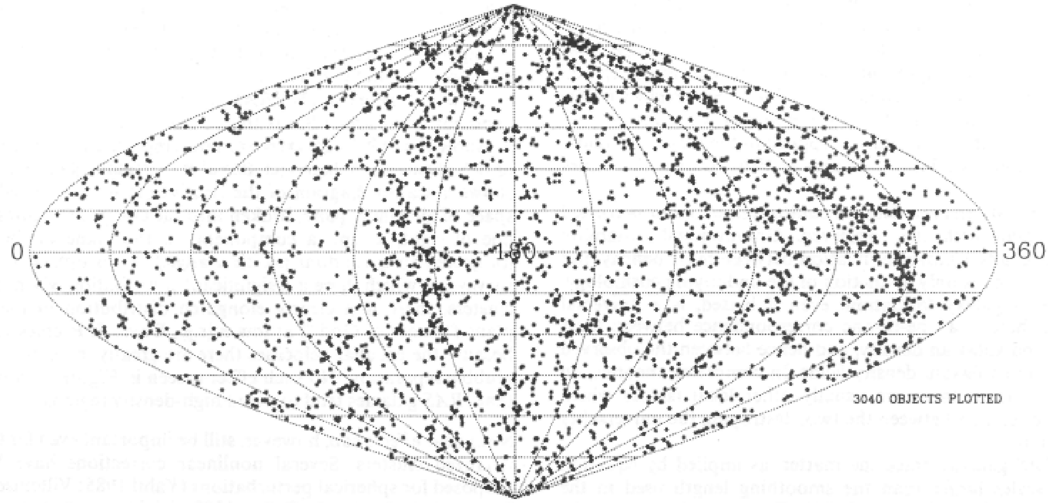

Figure 3. *The distribution in the sky of galaxies in the IRAS* 1.9*Jy redshift survey, including random galaxies in the masked region 'cloned' from neighbouring regions. From Yahil et al. (1991)*

(1991) 'cloned' galaxies from the regions neighbouring the masked region, thus ensuring continuity of structure across the Galactic plane. Figure 3, from Yahil et al (1991), shows the distribution of galaxies in the sky from the IRAS 1.9 Jy redshift survey used in their reconstruction, including the cloned galaxies in the masked region.

In recent years a more sophisticated statistical technique has been developed to improve further the treatment of the masked region. This approach again uses the idea of the *Wiener filter* (Wiener 1949), and can be regarded as a Bayesian approach to the problem – using the observed variations outside of the mask to define a prior model for the all-sky variations (Fisher et al. 1995b; Zaroubi et al. 1995). A similar statistical formalism has also been used to reconstruct the temperature distribution of the cosmic microwave background radiation behind the Galactic Plane (Bunn, Hoffman and Silk 1996).

4.4 The impact of non-linear effects: Triple valued zones

The iterative procedure outlined above uses eq. (26) to compute corrections to the redshift space distribution, but as we have already remarked eq. (26) is strictly valid only in the linear regime, where $\delta << 1$. How does one handle the situation when the linear approximation begins to break down? We will return to non-linear effects in detail in Section 4.5, but in the context of our iterative procedure we can easily see how they will already manifest themselves in a problematic way.

Figure 4 is a cartoon diagram sketching the relation between distance and redshift along a particular line of sight close to an overdense region in the survey. The gravitational effect of the overdensity induces a positive radial peculiar velocity for galaxies in front, and a negative radial peculiar velocity for galaxies behind the overdensity.

For a sufficiently small overdensity (or for a line of sight which does not directly cross the overdense region) the redshift-distance relation will deviate from the linear form expected for pure Hubble expansion (shown by the dotted line in Figure 4) but will still be monotonically increasing. As the size of the overdensity (and/or the proximity to it) increases, however, a redshift-distance relation similar to the solid curve will be obtained.

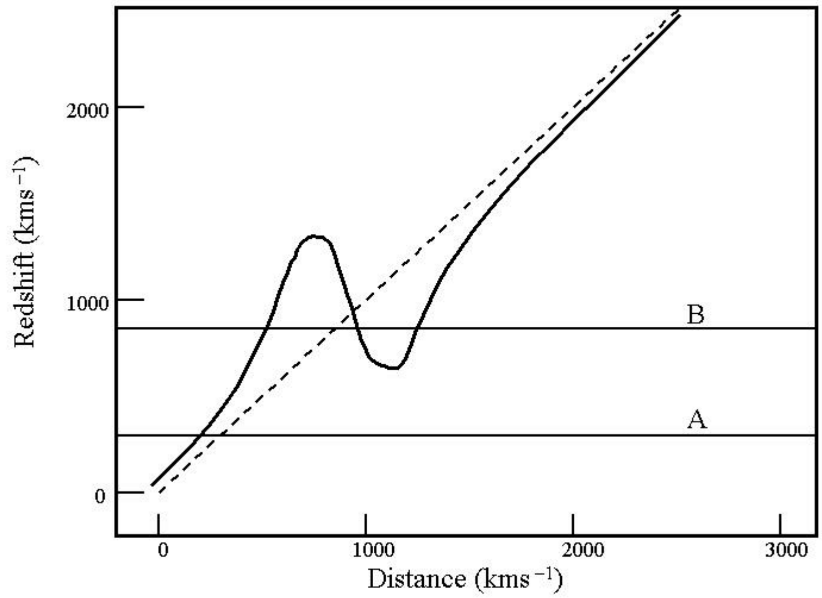

Figure 4. *Schematic illustration of the problem of 'triple valued zones' in non-linear evolution. The solid curve shows the relation between redshift and distance along a particular line of sight close to an overdensity in the matter distribution. At observed redshift A a unique distance may still be inferred, but at redshift B galaxies at three distinct distances along the line of sight have the same observed redshift.*

Thus at observed redshift A, for example, a unique distance may still be inferred; at redshift B, on the other hand, galaxies at three distinct distances along the line of sight have the same observed redshift. The obvious question arises: which distance should one adopt?

An iterative reconstruction scheme based on linear theory alone has no exact means of dealing with such triple valued zones. The approach adopted by e.g. Yahil et al. (1991) and subsequent authors has been to assign a distance to each galaxy probabilistically, drawn from the three computed possible solutions, so that the line of sight galaxy distribution matches in a statistical sense the reconstructed underlying density field from which it is sampled. In other words, one builds into the reconstruction a model for $p(r|cz)$, the probability distribution for the true galaxy distance, given the observed redshift. A more sophisticated version of this approach – known as the VELMOD maximum likelihood analysis – has recently been developed (Willick and Strauss 1998).

4.5 Relating the galaxy and mass density fields: Linear biasing?

Perhaps the most significant approximation in eqs. (25) and (26) is the assumption that galaxies are faithful tracers of the mass density field. On a very basic level this assumption is clearly false: we developed the theory of structure formation assuming a smooth mass density, while galaxies are sampled sparsely at discrete locations. The question remains, however: even with a 'good' estimate of $\delta_g(\mathbf{r})$ provided by a densely sampled all-sky redshift survey, to what extent can we assume that $\delta_g(\mathbf{r}) = \delta(\mathbf{r})$ – or, as the problem is usually expressed, to what extent does galaxy light trace mass?

Kaiser (1984) raised this question in the context of galaxy formation models and showed that, on the (reasonable) assumption that galaxies form at the peaks of the mass density field, then galaxy clustering will be stronger than the clustering of the mass distribution. Expressed in more formal statistical language, the *two-point correlation function* of the galaxy distribution (which measures the mean excess number of galaxy pairs with a given spatial separation, compared to the expected number of pairs in the absence of galaxy clustering) has a higher amplitude – indicating stronger clustering – than the correlation function of the mass distribution. Kaiser considered the case where galaxies form at peaks in the mass distribution above a certain, fixed, threshold, and showed that in this case the following simple relation holds

$$\delta_g(\mathbf{r}) = b\delta(\mathbf{r}) \tag{32}$$

where b is a constant related to the galaxy formation threshold.

Kaiser's model introduced the concept of 'biased galaxy formation', and the constant b is known as the linear bias parameter. While it is widely recognised that the threshold picture of how and where galaxies form is a gross oversimplification, the adoption of a linear treatment of galaxy bias has been a very popular one – not least because it can be very easily incorporated into the basic theoretical framework summarised in Section 3.2. In short, if we assume $\delta_g(\mathbf{r}) = b\delta(\mathbf{r})$ then we can re-write eqs. (25) and (26) as

$$\frac{\nabla \cdot \mathbf{v}}{a_0 H_0} = -\beta\, \delta_g \tag{33}$$

and

$$\mathbf{v}(\mathbf{r}) = \beta\, \frac{H_0}{4\pi} \int \frac{d^3r' \delta_g(\mathbf{r}')(\mathbf{r}' - \mathbf{r})}{|\mathbf{r}' - \mathbf{r}|^3} \tag{34}$$

where we have written

$$\beta = \frac{\Omega_0^{0.6}}{b} \tag{35}$$

Thus, the task of constraining Ω_0 from a comparison of the density and velocity fields becomes instead the task of constraining β. A great deal of work has been carried out in recent years testing the linear bias assumption (e.g. exploring the dependence of b on galaxy morphology and scale) and considering the possible application of reconstruction methods to measure nonlinear biasing – see for example Coles and Lucchin (1995) and Coles (1997) for a general introduction, and Dekel and Lahav (1999) and Sigad, Branchini and Dekel (2000) for recent perspectives. Such reconstruction analyses are in their infancy, however (although greater progress has been made in the statistical analysis of galaxy clustering as a probe of nonlinear biasing: see e.g. Verde et al. 1998; Verde, Heavens and Matarrese 2000; Scoccimarro et al. 2001) and in the remainder of our discussion of velocity and density reconstruction we shall restrict ourselves to the linear biasing model.

4.6 Beyond Linear Theory: The Zel'dovich Approximation

In analysing the evolution of cosmic structure in terms of a fluid description, one can adopt either a *Lagrangian* or *Eulerian* formulation. In the former case one defines a coordinate system which is 'attached' to the fluid elements, so that the Lagrangian coordinates of the elements remain fixed as the fluid evolves; in the latter case one's coordinate system is attached to points in space, with respect to which the fluid elements will move as the fluid evolves. Comoving coordinates are in some sense a hybrid of the two, since the comoving coordinates of the homogeneous background cosmology remain fixed as the Universe expands, but the evolving fluid which is a perturbation on the background model contains elements whose position and velocity change.

Linear perturbation theory makes the assumption that the comoving positions of the fluid elements change negligibly as the Universe expands, so that structures grow simply according to the linear growth factor, f, of eq. (23). Zel'dovich (1970) introduced an important approximation which extended linear theory in a powerful, and rather elegant, manner. The Zel'dovich approximation assumes that the difference between the Lagrangian position (usually denoted by $\mathbf{q}$) and Eulerian position ($\mathbf{x}$) of a fluid element may be written as the product of a purely time-dependent function and a purely spatially-dependent function, i.e.

$$\mathbf{x}(\mathbf{q}) = a(t)\left[\mathbf{q} + D_1(t)\psi(\mathbf{q})\right] \tag{36}$$

where $D_1(t)$ is the growing mode which appeared in eq. (19) and ψ is proportional to the gradient of the gravitational potential. Thus we see that the Eulerian position is simply the Hubble expansion, plus a separable perturbation.

The Zel'dovich approximation is very useful, in that it gives an excellent approximation to the true evolution of the velocity and density field into the mildly non-linear regime (roughly to δ of order 5) – as has been verified extensively by numerical simulations (see e.g. Sahni and Coles 1995; Dekel et al. 1999). It remains an excellent approximation so long as there remains a one-to-one mapping between the initial and final Eulerian positions of the fluid elements – i.e. so long as the trajectories of fluid elements do not intersect ('shell crossing'). Its usefulness in the context of dynamical reconstruction lies specifically in providing mildly non-linear versions of eqs. (25) and (26), thus allowing the density and velocity fields to be related on smaller scales than permitted in linear theory.

4.7 Directly mapping redshift space to real space

One of the main drawbacks of the simple iterative reconstruction scheme outlined in Section 4.1 is that it is computationally intensive. Several attractive alternatives have gained in popularity in recent years, which involve establishing a direct, non-iterative, relation between the dynamical fields in real space and redshift space.

The first direct approach which we consider is based on the fact that – as we have just seen in Section 4.5 – we can establish a unique one-to-one mapping (the Zel'dovich approximation) between the initial and final positions of galaxies which is valid up until shell crossing occurs. Assuming that the peculiar velocity field is *irrotational* (a reasonable assumption on large scales, since in linear theory the growing mode, D_1 in eq. (19), is indeed irrotational) one can then write down a Jacobian for the transformation between the initial galaxy distribution in real space and the final galaxy distribution in redshift space. The irrotationality assumption implies that the peculiar velocity field can be written as the gradient of a scalar velocity potential, Φ, a differential equation for which can be obtained from the Jacobian.

Nusser and Davis (1994) developed this approach – known as the ITF method – by expanding the density field and velocity potential (both in redshift space) in terms of spherical harmonics, producing the differential equation

$$\frac{1}{s^2}\frac{d}{ds}\left(s^2\frac{d\Phi_{lm}}{ds}\right)-\frac{1}{1+\beta}\frac{l(l+1)}{s^2}\Phi_{lm}=\frac{\beta}{1+\beta}\left(\delta_{lm}-\frac{1}{s}\frac{d\log\phi}{d\log s}\frac{d\Phi_{lm}}{ds}\right) \tag{37}$$

where s is the redshift space radial coordinate and ϕ is the radial selection function defined in eq. (29) – clearly selection effects have an impact here in the same way as they did for the iterative solution of eq. (26). One can solve eq. (37) for the spherical harmonic coefficients, Φ_{lm}, on a given shell in redshift space, and then obtain the (β dependent) peculiar velocity field by differentiation of the velocity potential. No iteration is required, although – since the method assumes the validity of the Zel'dovich approximation – it is incompatible with the existence of triple valued zones, and thus cannot be applied on small scales.

A related approach was adopted in Fisher et al. (1995b), where the density field was expanded in angular spherical harmonics and radial spherical Bessel functions – although this time assuming linear theory. Again one may establish the (β dependent) relationships between the expansion coefficients in real space and redshift space, taking account of the radial selection function and the angular mask of the redshift survey, and applying a Wiener filter to reduce the impact of shot noise. Rigorous testing of the reconstruction methods was carried out using mock redshift surveys generated from n-body simulations.

A comparison of 'true' and reconstructed velocities showed that the ITF method (Zel'dovich approximation + 2-D spherical harmonics on radial shells) and Fisher et al. method (Linear theory + Wiener filtered 3-D spherical harmonics) gave very similar results, and both were clearly superior to the iterative reconstruction scheme. Further development of the 'redshift space to real space operator' approach, using a spherical harmonic decomposition of the density and velocity field, can be found in Taylor and Valentine (1999).

Due to the presence of the radial and angular selection effects, the spherical harmonics and spherical Bessel functions no longer provide an orthogonal set of basis functions for the decomposition of the density field. This introduces coupling between the different modes of the expanded density field, and means that one cannot solve separately for each mode. However, the problem is still reasonably tractable since the redshift space distortions produced by the radial peculiar velocities and the flux limit affect only the radial modes, while the angular mask affects only the angular modes. An interesting alternative approach, which preserves the orthogonality properties of the expansion coefficients, was considered in Schumacher (2000). Here a Gram-Schmidt orthogonalisation procedure was applied to the redshifts and angular positions of galaxies in the PSCz catalogue in order to generate a new, fully orthogonal, set of basis functions on the 'masked' space (i.e. including the angular and radial selection effects directly in the orthogonalisation procedure). This analysis was closely based on a similar treatment of the 'masked' sky maps of the microwave background radiation, first proposed by Gorski (1994).

Another direct method of inferring the real space density and velocity field, proposed by Peebles (1990) and further developed by Giavalisco et al. (1993), is based on the *least action principle* and is (uniquely among the techniques discussed in this article) suitable for application to a discrete n-body system. One can derive the exact equations of motion for a multi-body gravitating system by finding the stationary points of the action. The method is exact, provided shell crossing has not occurred, and converges very quickly. It was first applied to redshift survey data in Peebles (1994) and Shaya, Peebles and Tully (1994). The least action approach has recently been developed further, via the Path Interchange Zel'dovich Approximation (PIZA) method of Croft and Gaztañaga (1997) and Valentine, Saunders and Taylor (2000).

4.8 Comparison with real data: independent distance indicators

The essential point of our discussion so far is that one may use all-sky redshift surveys to reconstruct the (β dependent) peculiar velocity and density fields, taking account of sparse sampling, radial and angular selection effects and (to some extent) non-linear evolution of the cosmic structure. The question then remains, how does one use the reconstructed fields to constrain the value of β? To do this requires *independent* information about δ and $\mathbf{v}$: we obtain this information from *redshift-independent distance indicators*. In the past decade many catalogues – containing thousands of galaxies with redshift-independent distance estimates – have been compiled, including the MAT sample (Mathewson, Ford and Buchhorn 1992); HM sample (Han and Mould 1992); CF sample (Courteau et al. 1993); Abell BCG sample (Lauer and Postman 1994); SCI sample (Giovanelli et al. 1997); KLUN sample (Theureau et al. 1997); nearby SNIa sample (Riess et al. 1997); MarkIII dataset (Willick et al. 1997); SBF survey (Tonry et al. 1997); SFI sample (Giovanelli et al. 1998); SMAC sample (Hudson et al. 1999); EFAR and ENEAR samples (Colless et al. 1999 and Wegner et al. 1999); SCII sample (Dale et al. 1999); Shellflow survey (Courteau et al. 2000); and LP10k survey (Willick 1999).

A discussion of the astrophysical basis of redshift-independent distance indicators lies beyond the scope of this article, although more details can be found in e.g. Hendry (1997) and Webb (1999). A typical example is the *Tully-Fisher relation*, which is appropriate to mention since it is based on a sound dynamical principle: that more massive spiral galaxies tend to rotate more rapidly. The Tully-Fisher relation is an empirical power-law relationship between the luminosity and rotation velocity (as deduced e.g. from the width of the 21cm emission line of neutral hydrogen in the disk) of spiral galaxies. By measuring the galaxy's rotation velocity at some specified location in the disk, one can use Tully-Fisher to estimate its luminosity, which one then compares with the observed brightness of the galaxy to infer its distance – by application of the inverse square law.

How can we use redshift-independent distance indicators to provide cosmological constraints? Consider, for example, the peculiar velocity field. From eq. (26), or other suitable reconstruction procedure, we can obtain $\mathbf{v}_\beta(\mathbf{r})$ – i.e. given a value for β we can predict the peculiar velocity field at any position in our survey volume. In particular, therefore, we can infer the *radial* peculiar velocity, $u_\beta(r_i)$ say, at the position of any observed galaxy. If $\hat{r}_i$ denotes an estimate of that galaxy's distance (expressed for convenience in kms^{-1}, equivalent to assuming $H_0 \equiv 1$), then an estimate of the radial peculiar velocity of the galaxy is simply

$$\hat{u}_i = cz_i - \hat{r}_i \tag{38}$$

One can then compare the (β dependent) predicted and estimated radial peculiar velocities to obtain in turn a maximum likelihood estimate (or confidence region) for β.

The principal drawback of this approach is that redshift-independent distance indicators such as Tully-Fisher are generally rather *noisy* – with typical distance error dispersions of about 20% for an individual galaxy. More problematically, this intrinsic scatter will introduce systematic errors when distance indicators are applied to estimate peculiar velocities. These systematic errors are intimately linked to a classic problem in statistical astronomy – known generically in the literature as *Malmquist bias*.

4.9 Malmquist bias of estimated distances and velocities

Malmquist (1920) considered the luminosity distribution of observable galaxies in a flux-limited sample, and concluded that the mean luminosity of observable galaxies would be systematically brighter than the mean of the underlying population of galaxies, since intrinsically fainter galaxies would be missing from the sample at large distances. This *bias* in the luminosity of observable galaxies has important consequences for estimating galaxy distances. A detailed discussion of this problem can be found in e.g. Hendry and Simmons (1994), Strauss and Willick (1995) and Teerikorpi (1997), and in what follows we present only a very brief summary of the salient statistical points.

One can understand the essence of the problem of Malmquist bias by considering the following scenario. Suppose one observes a spiral galaxy with true distance , $r_{\rm true}$, and uses e.g. the Tully-Fisher relation to obtain an estimate, $\hat{r}$, of that true distance. Given the intrinsic Tully-Fisher scatter, it is likely that $\hat{r}$ will differ significantly from $r_{\rm true}$. What, then, is $p(r_{\rm true}|\hat{r})$, the conditional probability distribution of $r_{\rm true}$, given $\hat{r}$?

One might reasonably suppose that, for a galaxy at a given *true* distance, the scatter in a properly calibrated distance indicator is equally likely to produce an under-estimated and over-estimated value of $\hat{r}$. More formally, we might assume that the conditional distribution of $\hat{r}$ given $r_{\rm true}$ has expectation value equal to $r_{\rm true}$, i.e.

$$E(\hat{r}|r_{\rm true}) = r_{\rm true} \tag{39}$$

However, we are interested in the conditional distribution of *true* distance given our estimated distance (i.e. we want to know where the galaxy *really* came from). We can relate $p(\hat{r}|r_{\rm true})$ and $p(r_{\rm true}|\hat{r})$ via Bayes' formula, so that

$$p(r_{\rm true}|\hat{r}) \propto p(\hat{r}|r_{\rm true})p(r_{\rm true}) \tag{40}$$

It immediately follows that, if $E(\hat{r}|r_{\rm true}) = r_{\rm true}$, one will **not** in general obtain $E(r_{\rm true}|\hat{r}) = \hat{r}$, because of the presence of the $p(r_{\rm true})$ term in eq. (40). Moreover, removing the bias which this term introduces strictly speaking requires knowledge of $p(r_{\rm true})$ – which is closely related to the very galaxy density field which we are trying to reconstruct. And, of course, from eq. (38) any residual bias present in our adopted galaxy distance will also impact on our estimated radial peculiar velocity – possibly leading to a spurious signature of large scale galaxy motion.

A number of different statistical approaches to correct for Malmquist bias have been proposed in the literature. Lynden-Bell et al. (1988) made the assumption of a uniform $p(r_{\rm true})$, thus defining *homogeneous Malmquist bias corrections* for their distance indicator. This led, however, to some debate in the literature over their detection of radial back inflow into their 'Great Attractor' region: could this detection have been merely the signature of uncorrected Malmquist bias? Landy and Szalay (1992) improved the uniform assumption in a novel way, using the distribution of galaxy distance *estimates* themselves to estimate $p(r_{\rm true})$. Many other authors (e.g. Hudson 1993; Willick 1994) have preferred to use other 'prior' data for $p(r_{\rm true})$, provided by e.g. iterative reconstruction of the IRAS density field as discussed in Section 4.1, although this approach had the disadvantage of weakening the independence of the redshift survey and distance indicator information. Newsam, Simmons and Hendry (1995) proposed a Monte-Carlo approach to bias correction which simultaneously addressed all the systematic errors present in reconstructing the dynamical fields; a similar treatment was developed in Freudling et al (1995).

Malmquist bias alone is no longer regarded as a serious problem for reconstruction techniques, and with more recent data consistent results have been obtained using different bias correction procedures and calibration methods. Suffice it to say, however, that careful attention to the impact of Malmquist bias remains a very important issue for most reconstruction methods, and that the adage "applying the wrong Malmquist bias correction is often worse than applying *no* bias correction" is a useful mantra.

4.10 The POTENT reconstruction procedure

The assumption that the peculiar velocity field is irrotational is the basis of another reconstruction procedure which has been studied intensively over the past decade: the POTENT method. First proposed by Bertschinger and Dekel (1988), POTENT is an extremely appealing – and rather simple – method in principle. As we have already remarked, if $\mathbf{v}$ is irrotational, then it may be written as the gradient of a scalar velocity potential, Φ. Hence, at any position, $\mathbf{r}$, we may write

$$\Phi(\mathbf{r}) = \int_0^{\mathbf{r}} \mathbf{v} \cdot d\mathbf{l} \tag{41}$$

where the line integral is path independent. In particular, then, we may choose a purely *radial* path, so that

$$\Phi(\mathbf{r}) = \int_0^{\mathbf{r}} u(r')dr' \tag{42}$$

where $u(r')$ is the radial component of the peculiar velocity at distance, r', along the line of sight to $\mathbf{r}$. Having evaluated $\Phi(\mathbf{r})$ one then obtains $\mathbf{v}(\mathbf{r})$ by differentiation.

The beauty of POTENT is, then, that one may evaluate the 3-D peculiar velocity field purely from knowledge of only the radial components, which are directly accessible from redshift-independent galaxy distance indicators. The drawback of POTENT, however, is that we need to know the radial component of $\mathbf{v}$ *everywhere*. This means that the practical implementation of POTENT requires a great deal of smoothing of the raw data. Our sparse and noisy estimates of the u_i at the positions of the galaxies in our survey must be interpolated onto a regular grid. This is achieved by *tensor window smoothing* (Dekel, Bertschinger and Faber 1990), in which a bulk flow velocity field model is fitted to the radial velocity estimates of galaxies in a large smoothing window centred on each grid point. A tensor approach is required since the radial velocities are not parallel across the smoothing window. Moreover, this means that the integration need not be restricted to radial paths. Simmons, Newsam and Hendry (1995) developed the MAXFLOW algorithm which adapts the standard POTENT procedure to include non-radial paths if, for example, this avoids a region where galaxy sampling is particularly poor. In practice, however, the tangential components of the fitted bulk flow velocity in each smoothing window are generally much noisier than the radial component, which means that the optimal integration path is rarely significantly non-radial.

The smoothing procedures and the nature of the data used when applying POTENT in practice introduce several possible sources of systematic error in the recovered peculiar velocity field, the two largest of which are Malmquist bias (due to scatter in the individual distance and peculiar velocity estimates) and sampling gradient bias (due to uneven sampling of the velocity field across each smoothing window). Since the precise magnitude of these biases is very sensitive to the details of the particular dataset to which POTENT is applied, a proper error analysis can only be carried out by Monte Carlo simulations (Dekel et al. 1999).

Having reconstructed the peculiar velocity field (Bertschinger et al. 1990; Dekel et al. 1999) one can then use e.g. eq. (25) to determine the mass overdensity field, δ, on a regular grid. Comparison with δ_g reconstructed from redshift survey data then permits the estimation of β (Dekel et al. 1993; Sigad et al. 1998). More recent implementations of this density-density comparison have extended the linear treatment to relate δ and $\mathbf{v}$ using the Zel'dovich approximation, or other non-linear schemes (Nusser et al. 1991). Again, the error analysis requires great care as the data points (the grid values of δ) are coupled not just by real correlations but also by noise, and a full Monte Carlo treatment is essential. Kolatt et al. (1996) build realistic n-body simulations which mimic the properties of the real galaxy data and use them to explore carefully different smoothing procedures and assess the impact of possible systematic errors at all stages of the velocity and density reconstruction and density-density comparison.

In summary, POTENT is a very attractive reconstruction method based on a very elegant idea, but is undermined by the sparse and noisy nature of its raw data, which necessitates highly complex smoothing and interpolation. Perhaps its most appealing feature is that it measures the mass density field directly – independent of any assumptions about galaxy biasing – because it uses galaxies as tracers of the velocity field and not of the density field. Dekel and Rees (1994) suggested that POTENT could, therefore, be used to place a robust lower limit on the value of Ω_0 by considering the divergence of the velocity field around voids in the galaxy distribution. This is because δ – which in linear theory is of course proportional to $\nabla \cdot \mathbf{v}$ – is bounded below by -1, so that the lowest measured value of $\nabla \cdot \mathbf{v}$ can place a robust lower limit on the constant of proportionality, $\Omega_0^{0.6}$, independent of biasing. Sparse sampling and data noise have prevented definitive application of this idea to date, but it remains an interesting possible future application of the POTENT method.

5 Conclusions

Although our aim in this article has been to describe reconstruction methods rather than results, it would be inappropriate to end without making at least some remarks about recent applications of these techniques to constrain cosmological models. We will restrict our attention to the linear bias parameter, β, which has attracted most attention in the literature.

Despite the considerable effort to test rigorously reconstruction methods and ensure their freedom from systematic error, there remains a lack of consensus in recently published determinations of β, with results divided roughly between methods which compare predicted and observed velocities, and those which compare predicted and observed densities. Chief examples of the latter category are POTENT-based comparisons using the Mark III catalogue of redshift-indpendent galaxy distance estimates and the density field reconstructed from the IRAS 1.2Jy redshift survey. Sigad et al. (1998, and references therein) favours a value of $\beta_I = \Omega_0^{0.6}/b_I \simeq 1$ from these analyses. (Here the subscript I denotes the fact that the comparison is between galaxies in the near infra-red part of the spectrum; galaxy biasing, and hence the value of b, will in general be wavelength dependent). Velocity-velocity comparisons, on the other hand, have generally favoured $\beta_I \simeq 0.5$ (Davis, Nusser and Willick 1996; Riess et al. 1997; Da Costa et al. 1998; Willick and Strauss 1998).

The origins of this significant discrepancy have not yet been elucidated (see for example Strauss 2000; Willick 2000). At least one of the reconstruction methods is suffering from some residual systematic effects. What are those systematic effects? Two facts would seem to give some indication. Firstly, lower β values have generally (although not always) also been found from statistical analyses of galaxy clustering in redshift space (Taylor and Hamilton 1996; Fisher and Nusser 1996; Tadros et al. 1999), which make no use of redshift-independent distance information, although some assumptions about the power spectrum of density fluctuations may remain. Secondly, recent development and application of the ROBUST method (Rauzy and Hendry 2000) gives $\beta_I = 0.6$. Although the details of this method are beyond the scope of this article, the salient point is that ROBUST uses redshift-independent distance indicators in a manner which requires no application of Malmquist bias corrections. Thus, the agreement between ROBUST and e.g. VELMOD (Willick and Strauss 1998) and ITF (Davis, Nusser and Willick 1996) suggests that the Malmquist bias corrections employed in the latter methods are indeed largely free from systematic error, and perhaps instead it is the sampling gradient biases associated with the POTENT smoothing procedure which are contributing to the higher β estimates from that method. Notwithstanding these remarks, it appears at least from the Monte Carlo analyses of Kolatt et al. (1996) and Dekel et al. (1999) that POTENT is *not* seriously contaminated by systematic error. Another possibility which must be faced is simply that the assumption of linear galaxy biasing is inadequate. Berlind, Narayanan and Weinberg (2000; 2001) are exploring the impact of various different non-linear, and even non-local, biasing schemes on reconstruction methods, and this work may yet shed light on the continuing β discrepancy. Certainly in the long term, POTENT-based methods offer an interesting means of disentangling the relationship between galaxies and mass, precisely because they treat galaxies as tracers of the velocity field – which responds to *all* gravitating mass, however it is clustered.

In summary, this article has hopefully made clear that the analysis of all-sky redshift surveys for the purpose of reconstructing the large scale density and velocity fields is a rapidly maturing topic, requiring sophisticated statistical machinery to cope with the sparse and noisy nature of the datasets used. Within the (possibly limited) framework of linear galaxy biasing, the best estimates of β to date have been obtained from infra-red surveys and indicate that $\beta_I \simeq 0.5$, consistent with the low Ω_0 values favoured by analyses of high redshift supernovae and the CMBR (see e.g. Tegmark and Zaldarriaga 2000) and with the assumption that IRAS galaxies appear to trace the mass distribution on large scales. This picture, while far from complete, appears to vindicate the gravitational instability paradigm, which is alive and kicking in Large Scale Structure.

Acknowledgements

The author is pleased to acknowledge many useful discussions with his collaborators in preparing this review – particularly Stéphane Rauzy, Elke Schumacher, John Simmons, Andrew Newsam and Kenton D'Mellow. The author would like to dedicate this article to the memory of Jeffery Willick, who was killed tragically in June 2000, after more than a decade of research in this field. Jeff Willick's outstanding work in the analysis of galaxy redshift and redshift-distance surveys – which has been extensively referenced throughout this article – has made an enormous, and lasting, contribution to our understanding of the large scale structure of the Universe, and his loss to the community is sorely felt.

References

Aaronson, M., et al., 1982, ApJS, 50, 241
Balian, R. and Schaefer, R., 1989, A&A, 220, 1
Bardeen, J., Bond, J.R., Kaiser, N. and Szalay, A., 1986, ApJ, 304, 15
Berlind, A., Narayanan, V.K. and Weinberg, D.H., 2000, ApJ, 537, 537
Berlind, A., Narayanan, V.K. and Weinberg, D.H., 2001, in prep.
Bertschinger, E. and Dekel, A., 1989, ApJ, 336, L5
Bertschinger, E., Dekel, A., Faber, S.M. and Burstein D., 1990, ApJ, 364, 370
Branchini, E., et al., 1999, MNRAS, 308, 1
Bunn, E.F., Hoffman, Y. and Silk, J., 1996, ApJ, 464, 1
Coles, P. and Lucchin, F., 1995, *Cosmology: The Origin and Evolution of Cosmic Structures*, (Chichester: John Wiley)
Coles, P., 1997, in *From Quantum Fluctuations to Cosmological Structures*, eds. D. Valls-Gabaud et al., ASP Conf. Ser. 126, 233
Colless, M., et al., 1999, MNRAS, 303, 813
Courteau, S., Faber, S.M., Dressler, A. and Willick J.A., 1993, ApJ, 412, L51
Courteau S., et al., 2000, in *Cosmic Flows 1999: Towards an Understanding of Large-Scale Structure*, eds S. Courteau et al., ASP Conf. Ser. 201, 17
Croft, R.A.C. and Gaztañaga, 1997, MNRAS, 285, 793
da Costa, L.N., et al., 1998, MNRAS, 229, 425
Dale, D.A., et al., 1999, ApJ, 510, 11
Davis, M., Nusser, A. and Willick,J.A., 1996, ApJ, 473, 22
Davis, M. and Peebles, P.J.E., 1983, ApJ, 267, 465
Dekel, A., Bertschinger, E. and Faber, S.M., 1990, ApJ, 364, 349
Dekel, A. and Rees, M.J., 1994, ApJ, 422, L1
Dekel, A., et al., 1993, ApJ, 412, 1
Dekel, A. and Lahav, O., 1999, ApJ, 520, 24
Dekel, A., et al., 1999, ApJ, 522, 1
Dekel, A. and Ostriker, J.P., 1999, *Formation of Structure in the Universe*, (Cambridge: CUP)
Dressler, A., et al., 1987, ApJ, 313, 42

Fisher, K.B., et al., 1995a, ApJS, 100, 69
Fisher, K.B., et al., 1995b, MNRAS, 272, 885
Fisher, K.B. and Nusser, A., 1996, MNRAS, 279, 1
Fixsen, D.J., et al., 1994, ApJ, 470, 38
Freudling, W., da Costa, L.N. and Pellegrini, P.S., 1994, MNRAS, 268, 943
Freudling, W., et al., 1995, AJ, 110, 920
Geller, M.J. and Huchra, J.P., 1989, Science, 246, 897
Giavalisco, M., Mancinelli, B., Mancinelli, P.J. and Yahil A., 1993, ApJ, 411, 9
Giovanelli, R. and Haynes, M.P., 1991, ARA&A, 29, 499
Giovanelli, R., et al., 1997, AJ, 113, 22
Giovanelli, R., et al., 1998, ApJ, 505, 91
Gorski, K.M., 1994, 430, L85
Groth, E.J. and Peebles, P.J.E., 1977, ApJ, 217, 385
Hamilton, A.J.S., 1998, in *The Evolving Universe*, ed. D. Hamilton (Kluwer Academic: Dordrecht), 185
Han, M., Mould, J.R., 1992, ApJ, 396, 453
Hendry, M.A., 1997, in *From Quantum Fluctuations to Cosmological Structures*, eds. D. Valls-Gabaud et al., ASP Conf. Ser. 126, 385
Hendry, M.A. and Simmons, J.F.L., 1994, ApJ, 435, 515
Hubble, E., 1929, Proc. Nat. Acad. Sci., 15, 168
Huchra, J.P., Davis, M., Latham, D. and Tonry, J., 1983, ApJS, 52, 89
Huchra, J.P., Geller, M.J., de Lapparent, V. and Corwin, H.G., 1990, ApJS, 72, 433
Hudson, M.J., 1993, MNRAS, 265, 43
Hudson, M.J., et al., 1999, ApJ, 512, 79
Kaiser, N., 1984, ApJ, 284, L9
Kaiser, N., 1987, MNRAS, 227, 1
Kaiser, N., et al., 1991, MNRAS, 252, 1
Kerscher, M., et al., 1997, MNRAS, 284, 73
Kirshner, R.P., Oemler, A. and Schechter, P.L., 1978, AJ, 83, 1549
Klypin, A. and Shandarin, S.F., 1993, ApJ, 413, 48
Kolatt, T., Dekel, A., Ganon, G. and Willick, J.A., 1996, ApJ, 458, 419
Kolb, E.W. and Turner, M.S., 1990, *The Early Universe*, (Redwood City: Addison-Wesley)
Krzewina, L.G. and Saslaw, W.C., 1996, MNRAS, 278, 869
Lahav, O., Lilje, P.B., Primack, J.R. and Rees, M.J., 1991, MNRAS, 251, 128
Landy, S.D. and Szalay, A., 1992, ApJ, 391, 494
Lauer, T.R. and Postman, M., 1994, ApJ, 425, 418
Liddle, A.R. and Lyth, D.H., 2000, *Cosmological Inflation and Large Scale Structure*, (Cambridge: CUP)
Lineweaver, C.H., 1997, in *From Quantum Fluctuations to Cosmological Structures*, eds. D. Valls-Gabaud et al., ASP Conf. Ser. 126, 185
Lineweaver, C.H., et al., 1996, ApJ, 470, 38
Loveday, J., Peterson, P.A., Maddox, S.J. and Efstathiou, G., 1994, ApJS, 107,201
Lynden-Bell, D., et al., 1988, ApJ, 326, 19
Maddox, S.J., 2000, in *Clustering at High Redshift*, eds. A. Mazure et al., ASP Conf. Ser. 200, 63
Maddox, S.J., Efstathiou, G., Sutherland, W.J. and Loveday, J., 1990, MNRAS, 243, 692
Malmquist, K.G., 1920, Medd. Lund. Astron. Obs. Ser. II, 22, 1
Mathewson, D.S., Ford, V.L. and Buchhorn, M., 1992, ApJS, 81, 413
Mould, J.R., et al., 2000, ApJ, 529, 786
Newsam, A.M., Simmons, J.F.L. and Hendry, M.A., 1995, A&A, 294, 627

Nusser, A., Dekel, A., Bertschinger, E. and Blumenthal, G.R., 1991, ApJ, 379, 6
Nusser, A. and Davis, M., 1994, ApJ, 421, L1
Peacock, J.A., 1999, *Cosmological Physics*, (Cambridge: CUP)
Peacock, J.A. and Dodds, S.J., 1994, MNRAS, 267, 1020
Peebles, P.J.E., 1990, ApJ, 362, 1
Peebles, P.J.E., 1993, *Principles of Physical Cosmology*, (Princeton: Princeton University Press)
Peebles, P.J.E., 1994, ApJ, 429, 43
Perlmutter, S., et al., 1999, ApJ, 517, 565
Riess, A.G., Davis, M., Baker, J. and Kirshner, R.P., 1997, ApJ, 488, 1
Rowan Robinson, M. et al., 1990, MNRAS, 247, 1
Sahni, V. and Coles, P., 1995, Physics Reports, 262, 1
Santiago, B.X., et al., 1995, ApJ, 446, 457
Saunders, W., et al., 2000, MNRAS, 317, 55
Scharf, C. and Lahav, O., 1993, MNRAS, 264, 439
Schechtman, S.A., et al., 1996, ApJ, 470, 172
Schumacher, E., *Optimal Representation of the Density Field from Redshift Surveys*, MSc Thesis, University of Glasgow, UK
Scoccimaro, R., Feldman, H., Fry, J.N. and Frieman, J.A., 2001, ApJ, 546, 652
Seldner, M., Siebers, B., Groth, E.J. and Peebles, P.J.E., 1977, AJ, 84, 249
Shaya, E.J., Peebles, P.J.E. and Tully, R.B., 1995, ApJ, 454, 15
Sigad, Y., et al., 1998, ApJ, 495, 516
Sigad, Y., Branchini, E. and Dekel, A., 2000, ApJ, 540, 62
Simmons, J.F.L., Newsam, A.M. and Hendry M.A., 1995, A&A, 293, 13
Strauss, M.A., 2000, in *Cosmic Flows 1999: Towards an Understanding of Large-Scale Structure*, eds S. Courteau et al., ASP Conf. Ser. 201, 3
Strauss, M.A., et al., 1992, ApJS, 83, 29
Strauss, M.A. and Willick, J.A., 1995, Physics Reports, 261, 271
Tadros, H., et al., 1999, MNRAS, 305, 527
Taylor, A.N. and Hamilton, A.J.S., 1996, MNRAS, 282, 767
Taylor, A.N. and Valentine, H., 1999, MNRAS, 306, 491
Teerikorpi, P., 1997, ARA&A, 35, 101
Tegmark, M. and Zaldarriaga, M., 2000, ApJ, 544, 30
Teodoro, L., 1999, *The Density and Velocity Fields of the Local Universe*, PhD Thesis, University of Durham, UK
Theureau, G., et al., 1997, A&A, 319, 435
Tonry, J.L., Blakeslee, J.P., Ajhar, E.A. and Dressler A., 1997, ApJ, 475, 399
Valentine, H., Saunders, W. and Taylor, A.N., 2000, MNRAS, 319, L13
van de Waygaert, R. and Icke, V., 1989, A&A, 213, 1
Verde, L., Heavens, A.F. and Matarrese, S., 2000, MNRAS, 318, 584
Verde, L., Heavens, A.F., Matarrese, S. and Moscardini, L., 1998, MNRAS, 300, 747
Vetollani, G., et al., 1997, A&A, 325, 954
Vogeley, M.S. et al., 1994, ApJ, 420, 525
Webb, S., 1999, *Measuring the Universe*, (Chichester: Springer Praxis)
Wegner, G., et al., 1999, MNRAS, 305, 259
Weinberg, S., 1972, *Gravitation and Cosmology: Principles and Applications of the General Theory of Relativity*, (New York: Wheeler)
White, M., Scott, D. and Silk, J., 1994, ARA&A, 32, 319
White, S.D.M., 1979, MNRAS, 186, 145
Wiener, N., 1949, in *Extrapolation and Smoothing of Stationary Time Series*, (New York: Wiley)
Willick, J.A., 1994, ApJS, 92, 1

Willick, J.A., 1999, ApJ, 516, 47
Willick, J.A., 2000, in *Cosmic Flows 1999: Towards an Understanding of Large-Scale Structure*, eds S. Courteau et al., ASP Conf. Ser. 201, 321
Willick, J.A., et al., 1997, ApJS, 109, 333
Willick, J.A. and Strauss, M.A., 1998, ApJ, 507, 64
Yahil, A., Strauss, M.A., Davis, M. and Huchra, J.P., 1991, ApJ, 372, 380
York, D.G., et al., 2000, AJ, 120, 1579
Zaroubi, S., Hoffman, Y., Fisher, K.B. and Lahav, O., 1995, ApJ, 449, 446
Zel'dovich, Y.B., 1970, A&A, 5, 84